OPEN ACCESS Freely available online

PLOS ONE

Reductive Reactivity of Iron(III) Oxides in the East China Sea Sediments: Characterization by Selective Extraction and Kinetic Dissolution

Liang-Jin Chen, Mao-Xu Zhu*, Gui-Peng Yang, Xiang-Li Huang

Key Laboratory of Marine Chemistry Theory and Technology, Ministry of Education, College of Chemistry and Chemical Engineering, Ocean University of China, Qingdao, China

Abstract

Reactive Fe(III) oxides in gravity-core sediments collected from the East China Sea inner shelf were quantified by using three selective extractions (acidic hydroxylamine, acidic oxalate, bicarbonate-citrate buffered sodium dithionite). Also the reactivity of Fe(III) oxides in the sediments was characterized by kinetic dissolution using ascorbic acid as reductant at pH 3.0 and 7.5 in combination with the reactive continuum model. Three parameters derived from the kinetic method: m_0 (theoretical initial amount of ascorbate-reducible Fe(III) oxides), k' (rate constant) and γ (heterogeneity of reactivity), enable a quantitative characterization of Fe(III) oxide reactivity in a standardized way. Amorphous Fe(III) oxides quantified by acidic hydroxylamine extraction were quickly consumed in the uppermost layer during early diagenesis but were not depleted over the upper 100 cm depth. The total amounts of amorphous and poorly crystalline Fe(III) oxides are highly available for efficient buffering of dissolved sulfide. As indicated by the m_0, k' and γ, the surface sediments always have the maximum content, reactivity and heterogeneity of reactive Fe(III) oxides, while the three parameters simultaneously downcore decrease, much more quickly in the upper layer than at depth. Albeit being within a small range (within one order of magnitude) of the initial rates among sediments at different depths, incongruent dissolution could result in huge discrepancies of the later dissolution rates due to differentiating heterogeneity, which cannot be revealed by selective extraction. A strong linear correlation of the m_0 at pH 3.0 with the dithionite-extractable Fe(III) suggests that the m_0 may represent Fe(III) oxide assemblages spanning amorphous and crystalline Fe(III) oxides. Maximum microbially available Fe(III) predicted by the m_0 at pH 7.5 may include both amorphous and a fraction of other less reactive Fe(III) phases.

Citation: Chen L-J, Zhu M-X, Yang G-P, Huang X-L (2013) Reductive Reactivity of Iron(III) Oxides in the East China Sea Sediments: Characterization by Selective Extraction and Kinetic Dissolution. PLoS ONE 8(11): e80367. doi:10.1371/journal.pone.0080367

Editor: Wei-Chun Chin, University of California, Merced, United States of America

Received July 27, 2013; **Accepted** October 10, 2013; **Published** November 15, 2013

Funding: This research was financially supported by the Natural Science Foundation of China (grant No. 41076045, and 41030858), the Shandong Province Natural Science Foundation (grant No. ZR2011DM003), and the Taishan Scholars Programme of Shandong Province. The funders had no role in study design, data collection and analysis, decision to publish, or preparation of the manuscript.

Competing Interests: The authors have declared that no competing interests exist.

* E-mail: zhumaoxu@ouc.edu.cn

Introduction

Iron (Fe) is the most abundant, redox-sensitive element on earth's surface. Its redox cycling in marine sediments has a profound influence on cycling and fate of carbon, sulfur, phosphorus, and a variety of trace elements [1–3]. In oxic marine sediments, secondary Fe phases (from weathering of Fe-bearing primary minerals) occur dominantly as Fe(III) oxides, hydroxides, and oxyhydroxides (collectively hereafter referred to as Fe(III) oxides) with a wide spectrum of mineralogy, crystallinity, morphology and chemical compositions. Therefore they usually display quite variable adsorption affinity and reduction reactivity [4–6]. For example, reactive Fe(III) oxides serve as an important sink for a large number of dissolved species, particularly phosphorus, arsenic and heavy metals through surface adsorption and incorporation [7,8], while their reductive dissolution in anoxic environments results in release of these elements into porewater and thus exerts a crucial control on benthic fluxes of these elements [8–10].

Chemical and microbial reductions are two competing mechanisms of Fe(III) oxide dissolution [11–13]. In organic matter (OM)-rich marine sediments where dissolved sulfide is readily available via sulfate reduction, chemical reduction of Fe(III) oxides by dissolved sulfide generally dominates over the microbial pathways since the former is thermodynamically more favored than the latter, whereas microbial Fe(III) reduction is more important in some other marine sediments where reactive Fe(III) is abundant and/or OM flux to the seabed is low to intermediate [1,13–17]. Rates of both chemical and microbial Fe(III) reductions are strongly dependent on the reactivity of Fe(III) oxides [4,18,19]. Thus quantitative characterization of Fe(III) oxide reactivity is of significance for understanding Fe cycles and its influences on diagenesis of many other interlinked elements.

Selective extraction and kinetic dissolution are two commonly used methods to characterize relative reactivity of various Fe(III) oxides. Sequential/selective extractions, which are initially for Fe speciation, can be used to deduce relative reactivity of Fe(III) oxides based on specific extractants used. For example, the refined sequential extraction procedure of Poulton and Canfield [20] can be used to discriminate easily reducible Fe(III) oxides (Fe_{ox1}) (mainly amorphous and poorly crystalline Fe(III) oxides such as ferrihydrite and lepodocrocite), reducible Fe(III) oxides (Fe_{ox2})

(mainly goethite, akaganéite and hematite), magnetite, and poorly reactive silicate Fe pool. One disadvantage of the extraction methods is that they are empirically defined and nonmineral specific, and that Fe(III) oxides in a single pool are assumed to be chemically homogeneous. Actually, each extraction step may describe a heterogeneous group of minerals with a wide range of reactivity as a single pool [21].

Postma [22] introduced a more quantitative kinetic method to describe the reactivity of Fe(III) oxide assemblages, which could offer a more detailed and nuanced picture of composition and reactivity of Fe(III) oxides in comparison with the conventional chemical extractions. Reductive reactivity of natural Fe(III) oxide assemblages with variable crystallinity and surface properties can be described by a reactive continuum, and a dissolution rate law of the Fe(III) oxide assemblages can be expressed as [22,23]:

$$\frac{J}{m_0} = k'(\frac{m}{m_0})^{\gamma} \quad (1)$$

where J is the reduction rate (μmol s^{-1}), k' is the apparent rate constant (s^{-1}), which can be used as a measure of reductive reactivity, m_0 is the theoretical initial mass of the reactive Fe(III) oxides, m is the remaining mass at a given time t, and γ is the apparent reaction order. Predicted γ value for ideal dissolving spheres or cubes is 2/3 [22]. In natural Fe(III) oxide assemblages γ is the function of crystal morphology, particle size distribution and reactive site density, and hence is a measure of the heterogeneity of the Fe(III) oxide assemblages undergoing dissolution [22,23]. Alternatively, Eq. (1) can be expressed in a logarithmic form:

$$\log(\frac{J}{m_0}) = \log k' + \gamma \log(\frac{m}{m_0}) \quad (2)$$

that provides straight lines with slope γ and intercept log k′. Integrating Eq. (1) for $\gamma \neq 1$ yields:

$$\frac{m}{m_0} = [-k'(1-\gamma)t + 1]^{\frac{1}{1-\gamma}} \quad (3)$$

Eq. (3) is based on the fraction of undissolved Fe(III) oxide (m/m_0) but the experimental data yield the dissolved amount m_t at time t. The amount of m can be obtained by subtracting m_t from m_0. For the convenience of data processing, Eq. (3) is converted to Eq. (4):

$$m_t = m_0[1-(1-k'(1-\gamma)t)^{\frac{1}{1-\gamma}}] \quad (4)$$

Optimized values of m_0, k' and γ can be simultaneously determined by fitting time-dependent dissolution data to Eq. (4) using a nonlinear least square procedure.

Time-dependent reductive dissolution of Fe(III) oxides by applying the kinetic method above has been commonly recorded at pH 3.0 using ascorbic acid as a reductant [21–27]. The kinetic method offers a standardized way to compare intrinsic reactivity of Fe(III) oxides, however, how to link the experimental measurement to the *in situ* reactivity of Fe(III) oxide reduction in natural environments remains to be solved [21]. The kinetic investigation has also been done in citrate-bicarbonate (CB) buffered ascorbate solution at pH 7.5 [24,28,29]. In comparison with the investigation at pH 3.0, the CB-buffered ascorbate is more selective to the most reactive fraction of Fe(III) oxides and thus offers another standard to characterize intrinsic reactivity of Fe(III) oxides. More significantly, kinetic parameters derived at pH 7.5 bear specific microbial implications: k' obtained at this pH, according to Hyacinthe et al. [24], can be used as a forecast proxy of microbial reactivity of Fe(III) oxides and m_0 as a maximum estimate of bioavailable Fe(III) present in sediments, even though, on average, bacteria can reduce only 65% of the estimated reactive Fe(III) because of the inaccessibility of a fraction of the Fe(III) pool to iron reducers due to physical occlusion [19,30].

In this contribution, selective extraction and kinetic dissolution were combined to investigate reductive reactivity of Fe(III) oxides in one gravity core collected from the East China Sea (ECS) inner shelf. The objectives of this study are: (1) to reveal the effects of early diagenesis on reductive reactivity of Fe(III) oxides based on depth-dependent variability of the three kinetic parameters, m_0, k' and γ; (2) to compare selective extraction and kinetic dissolution with regard to the reactivity of Fe(III) oxides.

Materials and Methods

Ethics statement

No official permission is required for the field studies because the study site is accessible to every Chinese citizen for scientific purposes and no protected species were sampled.

Study area and sampling

The ECS is one of the world's largest shelf seas (Fig. 1). Annually it receives 5×10^8 tonnes of terrestrial particulates [31,32], mainly from the Yangtze River, the third longest river in the world. A large amount of fine-grained particulates is transported southward along the coast driven by the Jiangsu and Zhejiang-Fujian Coastal Currents, and trapped in the inner shelf by the blocking of the northward Warm Taiwan Current offshore, developing an elongated inner-shelf mud wedge from the Yangtze River mouth into the Taiwan Strait [33]. The shelf sediment, particularly the inner shelf mud, is an important sink for Fe [34,35]. Chemical reduction of reactive Fe(III) in the sediment plays an important role in sulfur diagenetic cycling [35–38], while microbial Fe(III) reduction is expected to be also important in OM decomposition [35,39–41].

One gravity core was collected at site DH7-1 (121.10°E, 27.23°N, water depth 30 m) during the cruise from October 11th to 28th, 2011 (Fig. 1). Upon retrieval, the gravity core (length 168 cm) was immediately sectioned at 3−5-cm intervals over the upper 45 cm and 10-cm interval below this depth in N_2 atmosphere. All the sub-samples were sealed in zip-lock plastic bags under N_2 atmosphere and frozen at −18°C until further handling.

Selective extractions

Accurately preweighed frozen sediments in duplicate were dried at 105°C until constant weight for determination of wet/dry weight ratios, which were used to express contents of extracted solid-phase Fe in μmol per gram dry sediment (μmol g^{-1}). To quantify Fe(III) oxide pools with different reactivity, three selective extractions were used for speciation of solid-phase Fe in 10 selected layers of the core (see Table 1 for the details). The extractions were carried out at room temperature, unless otherwise stated.

Acidic hydroxylamine extraction. This extraction was carried out following Lovley and Phillips [42] to estimate amorphous Fe(III) oxides. Under N_2, 25 mL of mixing solution containing 0.25 M HCl and 0.25 M hydroxylamine was added to preweighed (~1 g) frozen sediments in triplicate for a 1-h extraction while shaking. After centrifugation (4800 rpm) and

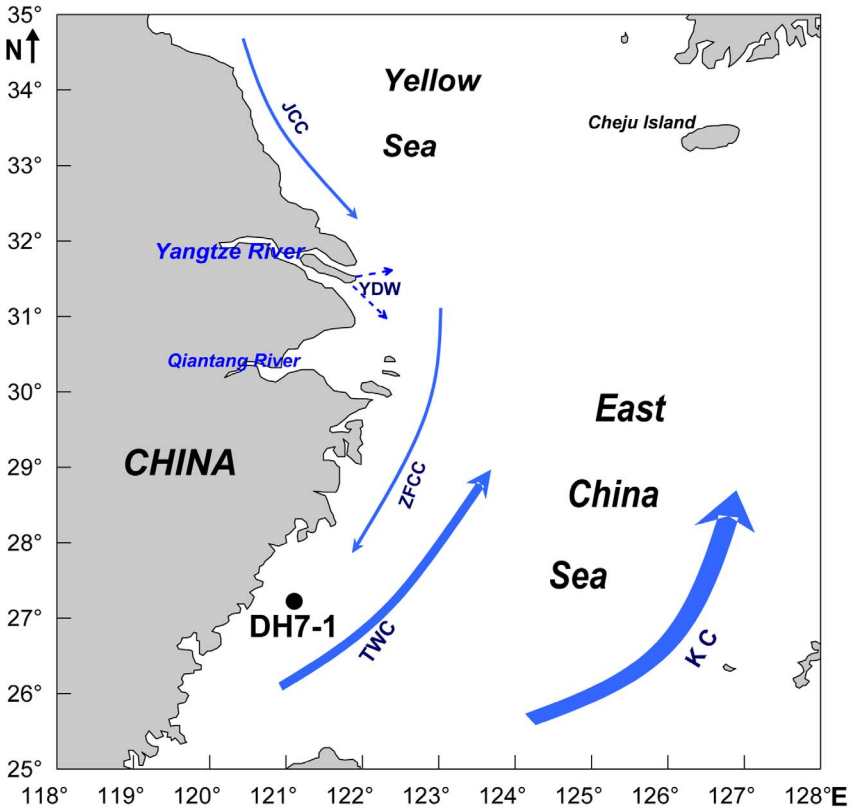

Figure 1. Regional ocean circulation patterns and sampling station in the East China Sea. JCC: Jiangsu Coastal Current; KC: Kuroshio Current; TWC: Taiwan Warm Current; YDW: Yangtze Diluted Water; ZFCC: Zhejiang-Fujian Coastal Current.
doi:10.1371/journal.pone.0080367.g001

filtration using polyether sulphone filtration membranes (0.22 μm, Membrana, Germany), supernatant was collected for Fe analysis. Another sub-sample was extracted by 0.25 M HCl solution (25 mL) by the same procedure as that described above. This extraction was used as a correction for H^+-promoted Fe dissolution in the acidic hydroxylamine extraction. An analysis of a standard solution containing both Fe^{2+} and Fe^{3+} and the blank sample indicated that the filters did not interfere with Fe concentrations and speciation in filtered samples.

Acidic oxalate extraction. Acidic oxalate is capable of extracting Fe(II)-bearing minerals such as Fe(II) sulfides (pyrite excluded), Fe(II) carbonates (siderite and ankerite), amorphous and poorly crystalline Fe(III), and magnetite [20,43]. Prior to determination of Fe(III) oxides, Fe(II) (pyrite excluded) was firstly

Table 1. Depth distributions of various solid-phase iron pools in gravity core DH7-1 of the East China Sea (unit: μmol Fe per gram dry sediment).

Depth (cm)	Acetate-Fe(II)	SD	Oxalate-Fe(III)	SD	BCD-Fe(III)	SD	Hydroxylamine-Fe(III)	SD	Magnetite	SD
1.5	40.1	0.05	132	16.5	191	0.54	16.7	0.02	41.7	3.07
5.5	40.6	0.26	138	8.09	142	0.07	12.1	0.17	40.3	4.26
10.5	41.2	0.87	131	15.0	154	0.87	8.88	0.83	36.2	2.46
15.5	42.0	0.31	124	2.05	189	8.55	7.70	0.19	39.4	6.29
30.5	42.4	0.83	124	10.4	157	10.6	7.24	<0.01	33.7	3.76
42.5	42.0	1.49	118	7.15	156	5.10	9.80	0.50	35.5	3.11
73	43.1	0.12	117	7.10	146	12.5	4.89	0.61	35.0	2.39
103	46.3	0.41	114	7.80	143	8.00	4.99	0.17	35.5	5.50
133	43.2	2.53	120	9.34	143	5.34	0.185	<0.01	39.1	2.78
163	43.8	0.57	113	1.47	136	6.57	1.29	0.04	45.2	4.39

SD: standard deviation.
Acetate-Fe(II): buffered acetate extractable Fe(II); oxalate-Fe(III): acidic oxalate extractable Fe(III); BCD-Fe(III): BCD-extractable Fe(III); hydroxylamine-Fe(III): Hydroxylamine extractable Fe(III).
doi:10.1371/journal.pone.0080367.t001

dissolved by buffered acetate extraction, which left most Fe (oxyhydr)oxides relatively unaffected [20]. Under N_2, 25 mL of NaAc-HAc buffer solution (pH 4.5) was added to preweighed frozen sediments (~0.5 g) (in triplicate) for a 24-h extraction while shaking. After centrifugation, supernatants were filtered for Fe^{2+} analysis. Residual sediment pellets were water-washed twice and then subjected to a 6-h extraction by 0.2 M oxalate (pH 3.2) for determination of Fe(III) oxides. After centrifugation and filtration, supernatants were collected for Fe analysis.

Bicarbonate-citrate buffered sodium dithionite (BCD) extraction. The extraction procedure followed de Koff et al. [44], which is a modified version of Mehra and Jackson [45] and Lord [46]. Under N_2, 20 mL of BCD solution (78 g/L sodium citrate, 9.3 g/L sodium bicarbonate, and 100 g/L sodium dithionite) was added to preweighed (~1 g) frozen sediments in triplicate for a 2-h extraction in water bath at 75°C while shaking. After centrifugation, supernatants were filtered for Fe analysis. The BCD is capable of extracting Fe(II) sulfides (pyrite excluded), amorphous and crystalline Fe(III) oxides, but only a fraction of magnetite (<15%) [20,47]. Fe(III) oxides extracted by the BCD were obtained as the difference between the BCD extraction and the buffered acetate extraction.

Magnetite extraction. Magnetite was separately estimated using the method of Poulton and Canfield [20] with a minor modification, that is, preweighed frozen sediments were sequentially extracted by BCD (2 h) at 75 °C and then by acidic oxalate (6 h), the oxalate-extractable Fe is an estimate of magnetite.

All extracted Fe was determined by colorimetry [48]. Variability (i.e., percent difference) among triplicates was 0.1−6.2% (mean 1.8%) for the buffered acetate extraction, <0.1−12.5% (mean 3.9%) for the acidic hydroxylamine extraction, 0.1−12.6% (mean 6.8%) for the acidic oxalate extraction, 0−11.2% (mean 3.8%) for the BCD extractions, and 7.4−16.0% (mean 10.1%) for the magnetite extractions.

Kinetic experiments

Kinetic experiments of Fe(III) oxide dissolution were undertaken at room temperature using ascorbic acid as a reductant at pH 3.0 and 7.5, respectively, by monitoring time-dependent Fe^{2+} release from the sediments. The experimental procedure at pH 3.0 was similar to Postma [22] and Larsen et al. [21]. Briefly, a preweighed frozen sediment (~4 g) was loaded into a reactor containing 1 L deoxygenated ascorbic acid solution (10 mM), which was pre-adjusted to pH 3.0 using dilute HCl. After being tightly sealed with a rubber stopper, the reactor was magnetically stirred and purged with N_2 during 12−27-h experiments to ensure a homogeneous and anoxic system. Fitted through the stopper were three outlets, one for sampling and the two others for gas in/out, and a pH electrode for pH monitoring. The pH was stabilized at 3.0 by adding dilute HCl with an autotitrator. The suspension was periodically sampled using 1-mL syringes and filtered (0.22 μm) directly into glass vials containing Na-acetate-buffered ferrozine solution for Fe determination by colorimetry [48]. At pH 3.0, H^+-promoted dissolution of Fe(II)-bearing minerals such as Fe(II) monosulfides and siderite ($FeCO_3$) is significant, while dissolution of Fe(III) oxides is negligible [23]. Thus kinetic dissolution in HCl solution (pH 3.0) was also carried out on another subsample as the correction for H^+-promoted Fe(II) dissolution in the ascorbic acid solution.

The experimental procedure at pH 7.5 was the same as that described above with the exception that the reductant was CB-buffered ascorbate (pH 7.5) [24,28]. In this case, H^+-promoted dissolution of Fe(II)-bearing minerals was negligible, and thus a correction was not needed.

Optimized values of m_0, k' and γ were simultaneously obtained by fitting the kinetic data to Eq. (4) using a nonlinear least squares procedure (Origin ver. 8.5). In what follows, where a discrimination is necessary, m_0, k' and γ obtained at pH 3.0 are denoted as $m_0(3.0)$, $k'(3.0)$ and $\gamma(3.0)$, and the ones obtained at pH 7.5 as $m_0(7.5)$, $k'(7.5)$ and $\gamma(7.5)$.

Note that not all the runs of the kinetic experiments were replicated due to tremendously huge workload. Only two selected runs at pH 3.0 and 7.5, respectively, were performed in duplicate to examine the reproducibility of the experiments. Results showed that variability (i.e., percent difference) for dissolved Fe^{2+} (i.e., m_t) between duplicates of the selected runs was less than 6%, however, m_0, k' and γ had larger variability (7−10%) due to error accumulation in the fittings.

Results

Pool sizes of selective extractions

The sizes of Fe(II) and Fe(III) pools are shown in Table 1 and Fig. 2. The hydroxylamine reducible Fe(III) oxides displayed a quick downcore decrease from 16.7 to 7.7 μmol/g in the upper 16 cm, and then a gradual decrease to very low values (0.19−1.3 μmol/g) below a depth of 130 cm. The oxalate extractable Fe(III) pool was in the range of 113−138 μmol/g and displayed an apparent downcore decrease in the upper 16 cm, below which only a small decrease was observed. The BCD-extractable Fe(III) pool was in the range of 136−191 μmol/g and exhibited a quick downcore decrease in the upper 11 cm. A peak value of the pool occurred at around 16-cm depth, below which a small decrease with depth was observed. Magnetite contents were in the range of 33.7−45.2 μmol/g with no clear depth variability. The average (38.3 μmol/g) is slightly lower than that for the ECS surface sediments (46.4 μmol/g) [35].

Kinetic parameters at pH 3.0 and 7.5

Representative curves of time-dependent Fe^{2+} release from the sediments at pH 3.0 and 7.5 are shown in Fig. 3. Optimized values of m_0, k' and γ are shown in Fig. 4. The values of $m_0(3.0)$, $k'(3.0)$ and $\gamma(3.0)$ were 23−57 μmol/g, $1.6-13.4\times10^{-4}$ s^{-1}, and 0.95−7.13, respectively. The values of $m_0(7.5)$, $k'(7.5)$ and $\gamma(7.5)$ were 14−29 μmol/g, $1-1.7\times10^{-4}$ s^{-1}, and 1.33−5.22, respectively. Although the m_0, k' and γ at pH 3.0 were larger than the corresponding values at pH 7.5, the three kinetic parameters at the two pHs displayed similar depth-dependent patterns. For example, all of the kinetic parameters exhibited maximum values in the surface sediments, a rapid decrease with depth to 16 cm, followed by a more gradual decline below 16 cm.

Discussion

Fe speciation by selective extractions

Hydroxylamine reducible Fe(III). Under acidic conditions, 1-h hydroxylamine extraction mainly targets amorphous Fe(III) oxides, and the extraction provides a simple and rapid technique to assess the availability of Fe(III) oxides for microbial reduction, albeit being underestimated [42]. The maximum of hydroxylamine reducible Fe(III) (16.7 μmol/g) in the surface sediments of the current study is comparable to the values for surface sediments in the Potomac Estuary (<20 μmol/g) [42], though the site of the current study has higher salinity (34−35‰) and sulfate concentration (26−28 mM) than the Potomac Estuary (salinity: 11‰, sulfate: 10−15 mM). The rapid downcore decrease in the hydroxylamine reducible Fe(III) in the upper 16 cm indicates a quick consumption through reduction. Although a variety of

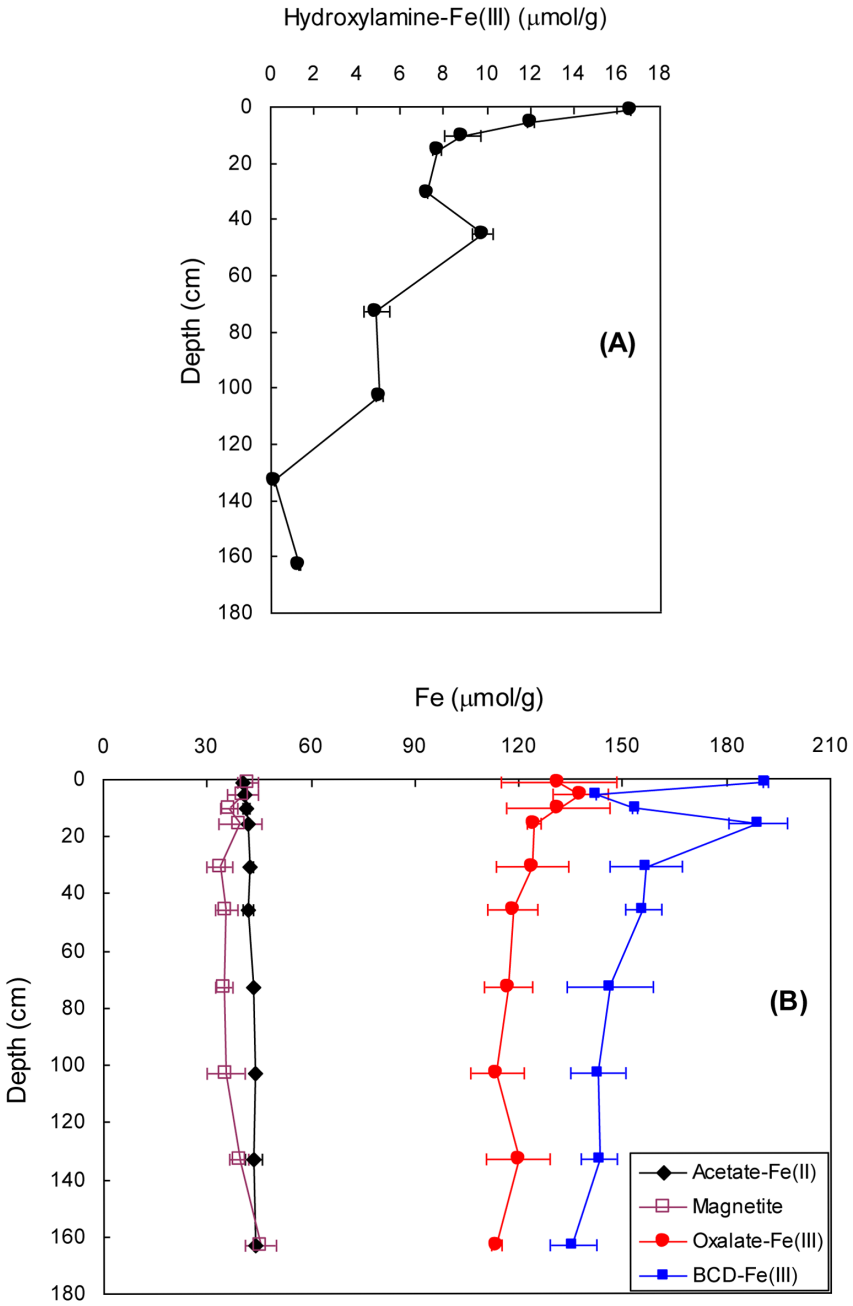

Figure 2. Depth profiles of extracted Fe (μmol per g dry sediment). (A) hydroxylamine-extractable ferric Fe (hydroxylamine-Fe(III)), (B) oxalate-extractable ferric Fe(III) (oxalate-Fe(III)), BCD-extractable ferric Fe (BCD-Fe(III)), buffered-acetate extractable ferrous Fe (acetate-Fe(II)), and magnetite. Error bars represent ±1 standard deviation.
doi:10.1371/journal.pone.0080367.g002

Fe(III) oxides, including poorly reactive sheet silicate Fe(III), are chemically and microbially reducible on wide timescales, highly reactive Fe(III) oxides, particularly amorphous Fe(III) phases, are usually consumed preferentially. The presence of acid volatile sulfides and pyrite (FeS_2) in the inner shelf sediments of the ECS suggests that chemical reduction has played an important role in Fe(III) reduction [35,37,40,49], while dissimilatory Fe(III) reduction may have also played a role, according to previous biogeochemical and microbiological observations [35,39-41]. The persistence of hydroxylamine reducible Fe(III) to a depth of around 100 cm in this study, albeit being at a low level, indicates that amorphous Fe(III) phases was not depleted over this depth interval. This is quite different from the findings of Lovley and Phillips [42], who found that hydroxylamine reducible Fe(III) in the Potomac Estuary sediments decreased rapidly with depth and became nearly exhausted below the upper 3 cm. The persistence of the Fe(III) pool at the deeper sediments of this study can be ascribed to small consumption of the pool by reaction with limited hydrogen sulfide. Limited availability of hydrogen sulfide in porewater of the sediments has been confirmed by previous studies, which suggested that sulfate reduction and thus sulfide production in the ECS shelf sediments was limited by generally

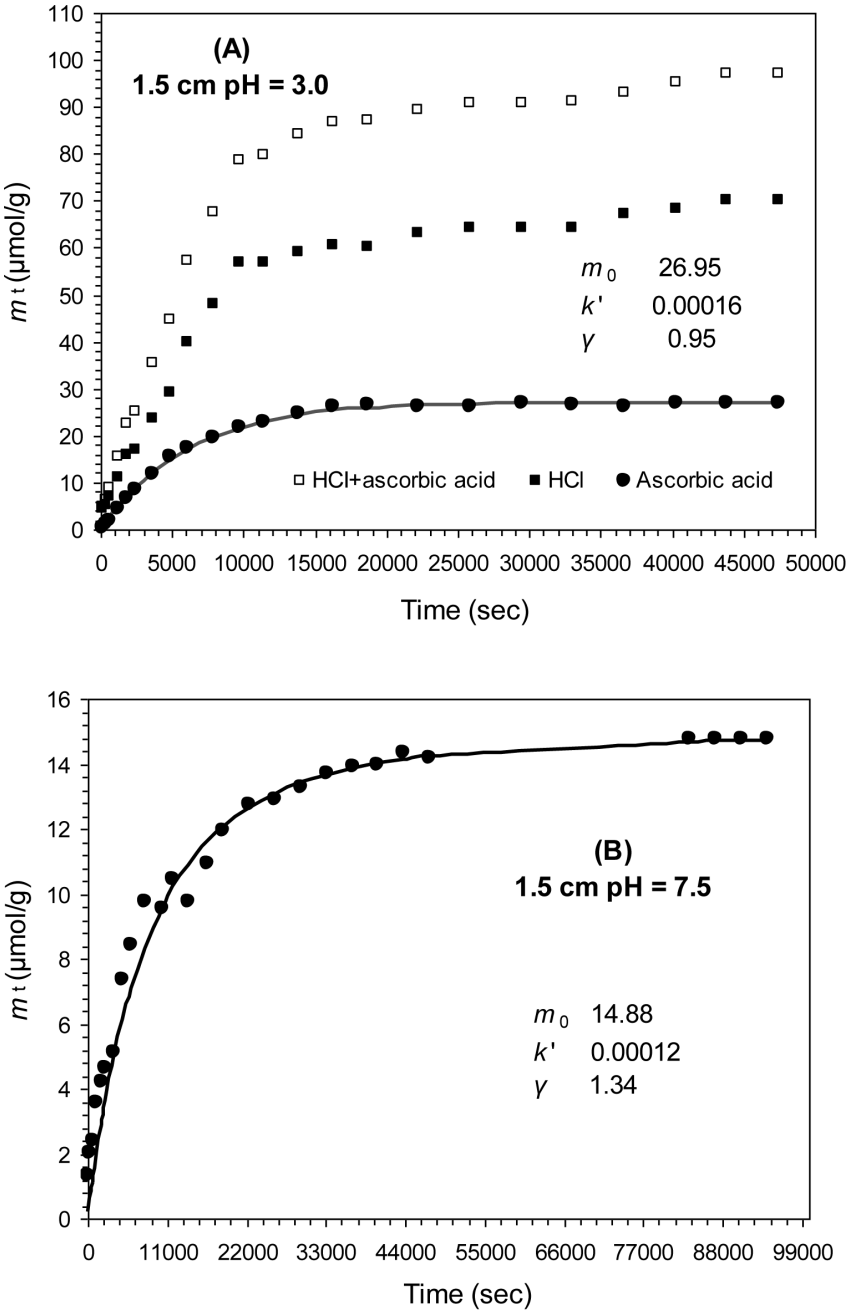

Figure 3. Representative curves of time-dependent release of Fe^{2+} from sediments (1.5 cm depth). (A) Fe^{2+} release in HCl solution at pH 3.0 (■) and in HCl + ascorbic acid solution at pH 3.0 (□). Fe^{2+} release by reductive dissolution (●) is obtained as the difference between the release in HCl + ascorbic acid solution and in HCl solution. (B) Fe^{2+} release in buffered ascorbate (pH 7.5). Solid lines in (A) and (B) are nonlinear least squares fits to equation 4.
doi:10.1371/journal.pone.0080367.g003

low degradability of OM and high redox potential caused by intensive physical reworking [37,40,49,50]. In the deeper layers, microbial Fe(III) reduction is expected to be insignificant, if any, because high activity of iron reducers is generally restricted to the upper suboxic/anoxic layers.

Acidic oxalate- and BCD-extractable Fe. In the present study, all Fe(II) sulfides (pyrite excluded) were extracted by buffered acetate prior to the oxalate extraction. Thus oxalate-extractable Fe can be used as an estimate of amorphous and poorly crystalline Fe(III) oxides plus magnetite. Magnetite is usually a minor mineral in modern marine sediments, but our previous study indicated that the ECS surface sediments have magnetite contents (25−74 µmol/g, with an outlier of 104 µmol/g) [35] higher than for many other marine sediments (<17.8 µmol/g) [51,52]. Magnetite contents in the core studied (33.7−45.2 µmol/g) are within the range for the ECS surface sediments [35].

The amounts of amorphous and poorly crystalline Fe(III) oxides can be estimated by subtracting magnetite content from the oxalate extraction. The estimated amounts of amorphous and

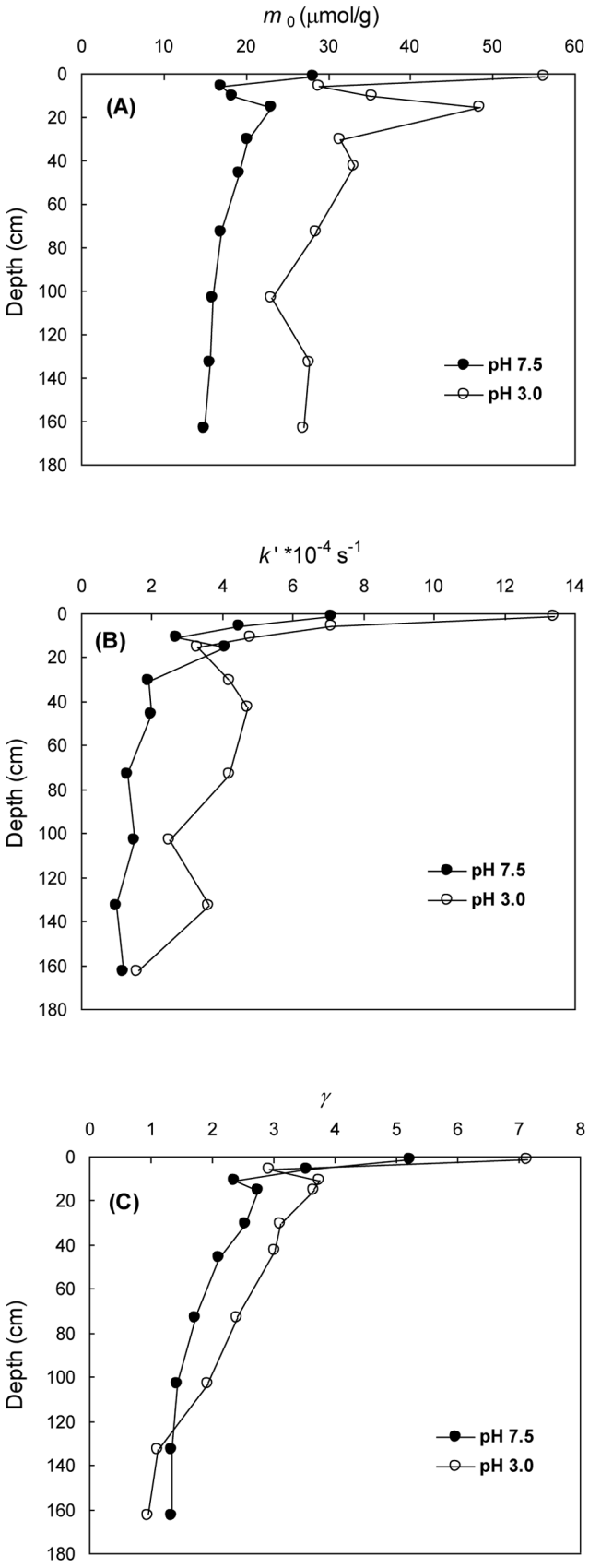

Figure 4. Depth profiles of m_0, k' and γ at pH 3.0 and 7.5. (A) m_0, (B) k', (C) γ.
doi:10.1371/journal.pone.0080367.g004

poorly crystalline Fe(III) oxides after correction for the magnetite were in the range of 68−98 μmol/g. Amorphous and poorly crystalline Fe(III) oxides are the major components of the Fe(III) pool responsible for quick buffering of dissolved sulfide in porewater [53,54]. The high amounts of this pool over the entire core imply that it has not been substantially consumed and is readily available for further buffering of dissolved sulfide. This is in agreement with our previous findings [40,50].

Contents of crystalline Fe(III) oxides (mainly goethite, akaganéite and hematite) and the total crystalline Fe oxides including magnetite can be estimated using the results of the BCD extractions, the oxalate extractions, and the magnetite. Estimated contents of crystalline Fe(III) oxides were 45–104 μmol/g and the total contents of crystalline Fe oxides including magnetite were 85−144 μmol/g. Both the BCD- and oxalate-extractable Fe(III) oxides displayed only a small downcore decrease and maintained high values at depth, suggesting that there has been only a small consumption of the two Fe(III) pools during long-term diagenesis. A subsurface (~16 cm depth) peak of the BCD-extractable Fe(III) is probably due to accumulation of some well crystalline Fe oxides at the redox interface due to aging of newly generated Fe(III) oxide phases given that oxalate-extractable Fe(III), mainly amorphous and poor crystalline Fe(III) oxides and magnetite, did not display a peak at similar depths.

Kinetic characterization of diagenetic effects on Fe(III) oxide reactivity

As shown in Fig. 4, depth-dependent variability of m_0, k' and γ at both pH 3.0 and 7.5 indicate that diagenesis has exerted a great impact on reactivity of Fe(III) oxides in the uppermost layer while a much less but persisting impact at depth. Maximum m_0, k' and γ occurring in the surface/subsurface layers is not unexpected because regeneration of highly reactive Fe(III) oxides by reoxidation of Fe^{2+} in the layers, particularly at the redox interface, is always active; on the other hand, intensive physical reworking causes mixing of surface/subsurface sediments and aging of Fe(III) oxides to varying extents due to repetitive resuspension, which is expected to render Fe(III) oxide assemblages enormously heterogeneous. In the ECS inner shelf, highly dynamic fluidized mud at the surface is expected to encourage upward diffusion and subsequent reoxidation of Fe^{2+} in the subsurface and surface sediments, as well as mixing and aging of Fe(III) oxides [49,50,56]. A similar phenomenon was also observed for manganese oxides in the North Sea sediments [55]. In addition, bioturbation by macrofauna may create diverse microenvironments and redistribute sediments and Fe(III) oxides [49], further enhancing the heterogeneity of Fe(III) oxide reactivity. The quick downcore decrease in m_0, k' and γ in the uppermost zone indicates preferential consumption of highly reactive Fe(III) oxides by chemical and/or microbial reduction, leaving more resistant and less heterogeneous residual Fe(III) phases behind. This is in agreement with the accepted notion that highly reactive Fe(III) oxides exhibit a quick downcore decrease in anoxic sediments and also in agreement with the result of the rapid downcore decrease in amorphous Fe(III) oxides quantified by the hydroxylamine extraction (Fig. 2). It should be pointed out that the reduction of Fe(III) oxides is not necessarily reflected in the profile of buffered-acetate extractable Fe(II) (Fig. 2B) because a large fraction of Fe(II) occurs as pyrite, which is non-extractable by buffered acetate.

The slow decrease in m_0 from 16 cm depth to the bottom indicates that the Fe(III) oxide pool has been subjected to a slow but persisting reduction over a long timescale, which can be ascribed to a combined result of progressive decrease in Fe(III) oxide reactivity and limited availability of dissolved sulfide to react

with the Fe(III) pools. The slow decrease in m_0 also resulted in a concomitant decrease in k' and γ. Coupling among the three kinetic parameters is illustrated by generally good linear correlations (t test, $p<0.05$) among them (except a weak correlation between $m_0(3.0)$ and $k'(3.0)$) (Fig. 5). The coupling is expected to be the result of diagenesis as the common driving force. Actually, it is hard to imagine that a similar coupling does occur in sediments where reactive Fe does not share the common origins and driving forces in cycling. It should be pointed out, however, that a similar coupling may not be observed in a short sediment core, and common diagenesis does not necessarily result in a linear coupling among the three parameters when some specific highly reactive Fe(III)-bearing minerals dominate the sediments. For example, a rapid downcore decrease in $m_0(7.5)$ in the subsurface layers of the Appels and Waarde sediments and a gradual decrease in the deeper layers (35−41 cm) were observed, however, $k'(7.5)$ and $\gamma(7.5)$ displayed no clear depth trend over the entire depth interval, due, at least, to abundant but highly varying contents of authigenic Fe(III)-P minerals, a highly reactive Fe(III)-bearing phase [24,28].

In comparison with a wide range of initial rates $k'(3.0)$ reported for Fe(III) oxide coated sands, soils, riverine and marine sediments ($10^{-7}-10^{-2}$ s^{-1}) [21,22,25–27,57], the change in the $k'(3.0)$ in the present study is small ($1.6-13.4\times10^{-4}$ s^{-1}). Also the $k'(7.5)$ values are in a small range ($1-1.7\times10^{-4}$ s^{-1}) and generally lower than the values for the Appels and Waarde sediments bearing highly reactive authigenic Fe(III)-phosphate minerals ($4.0-19.3\times10^{-4}$ s^{-1}) at the corresponding depths [24,28]. The range of the $\gamma(3.0)$ (0.95−7.13) in the present study is larger than that reported in the literature (0.79−5.14) [21,22,25–27,57], while the $\gamma(7.5)$ (1.33−5.22) is in a narrower range than that reported in the literature ($\gamma(7.5)=1.1-10$) [24,28].

The plots of $-\log(m/m_0)$ versus $-\log(\mathcal{J}/m_0)$ (Fig. 6) can illustrate temporal evolution of dissolution rate as Fe(III) oxide dissolution is in progress [21,22]. Figure 6 can also provide some mineralogical information of Fe(III) oxides, in a relative sense, by comparing with the reactivity of some synthetic Fe(III) oxides. For this purpose, the reactivity of some synthetic Fe(III) oxides is also shown in Fig. 6. At pH 7.5, only ferrihydrite and amorphous $Fe(PO_4)_{0.7}$ (Fig. 6B) are shown because they are the only synthetic phases whose reactivity at this pH is available [24,29]. The k'(pH 3.0) in the uppermost sediments is slightly higher than that for synthetic ferrihydrite while the k'(pH 3.0) in the deeper sediments is between that for synthetic ferrihydrite and lepidocrocite. This indicates that Fe(III) oxides in the uppermost sediments have higher reactivity than synthetic ferrihydrite. In the deeper layers, however, the reactivity decreased to be lower than for synthetic ferrihydrite but still higher than for lepidocrocite. The $k'(7.5)$ values over the upper 16 cm (with the exception at 10.5 cm depth) are within the range for synthetic ferrihydrite (aging for 3 to 11 days), while the $k'(7.5)$ in the deeper sediments is much lower than that for ferrihydrite. Over the entire depth interval the $k'(7.5)$ is lower than that for amorphous $Fe(PO_4)_{0.7}$. It should be pointed out that the reactivity of the Fe(III) oxide assemblages is 2−3 orders of magnitude higher than that for synthetic ferrihydrite that has been subjected to de-watering and aging to varying extents ($k'(7.5)=0.3-4.7\times10^{-6}$ s^{-1}) [29].

After 90% (i.e., $-\log(m/m_0)=1$) of the Fe(III) oxides in the upper sediments has dissolved, dissolution rates of the residual phases at pH 3.0 and 7.5 decreased by 7 and 5 orders of magnitude, respectively, relative to their corresponding initial rates. This is due to great heterogeneity of the Fe(III) oxide assemblages, comprising both highly reactive and more resistant phases. Similarly, Van der Zee and van Raaphorst [55] found a change up to 6 and 9 orders of magnitude for manganese oxides in

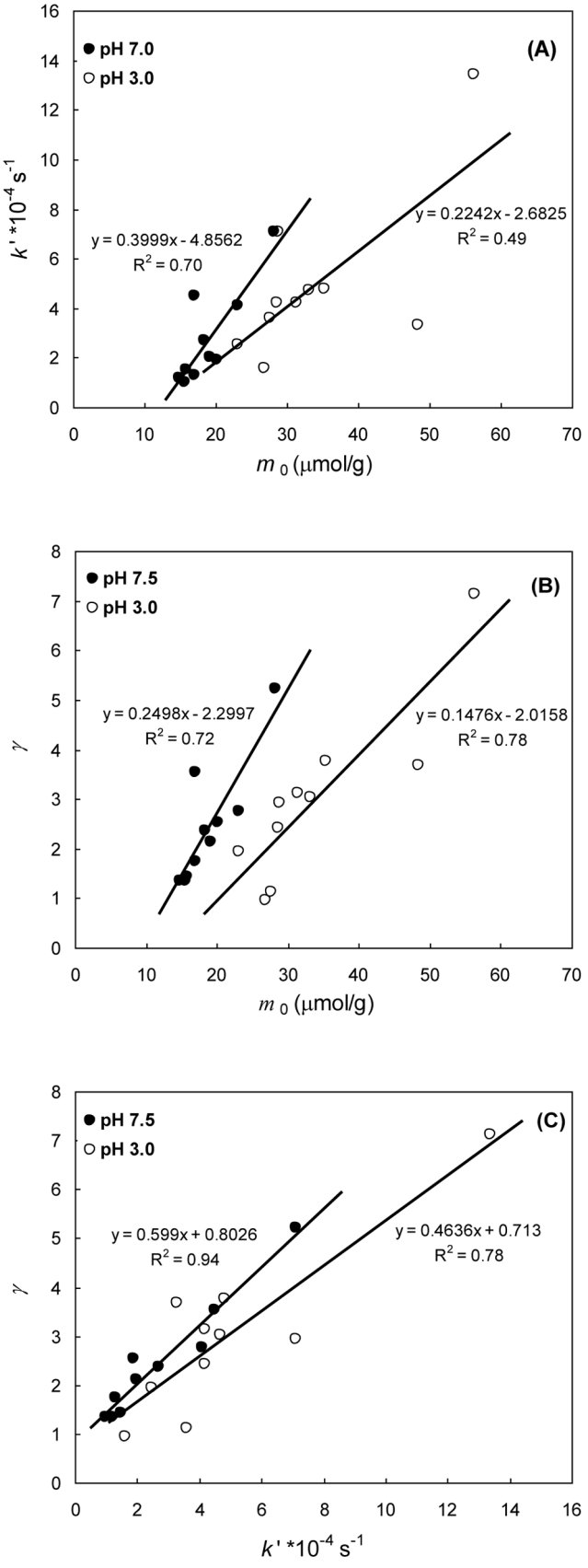

Figure 5. Correlations of m_0 vs. k' (A), m_0 vs. γ (B), and k' vs. γ (C).
doi:10.1371/journal.pone.0080367.g005

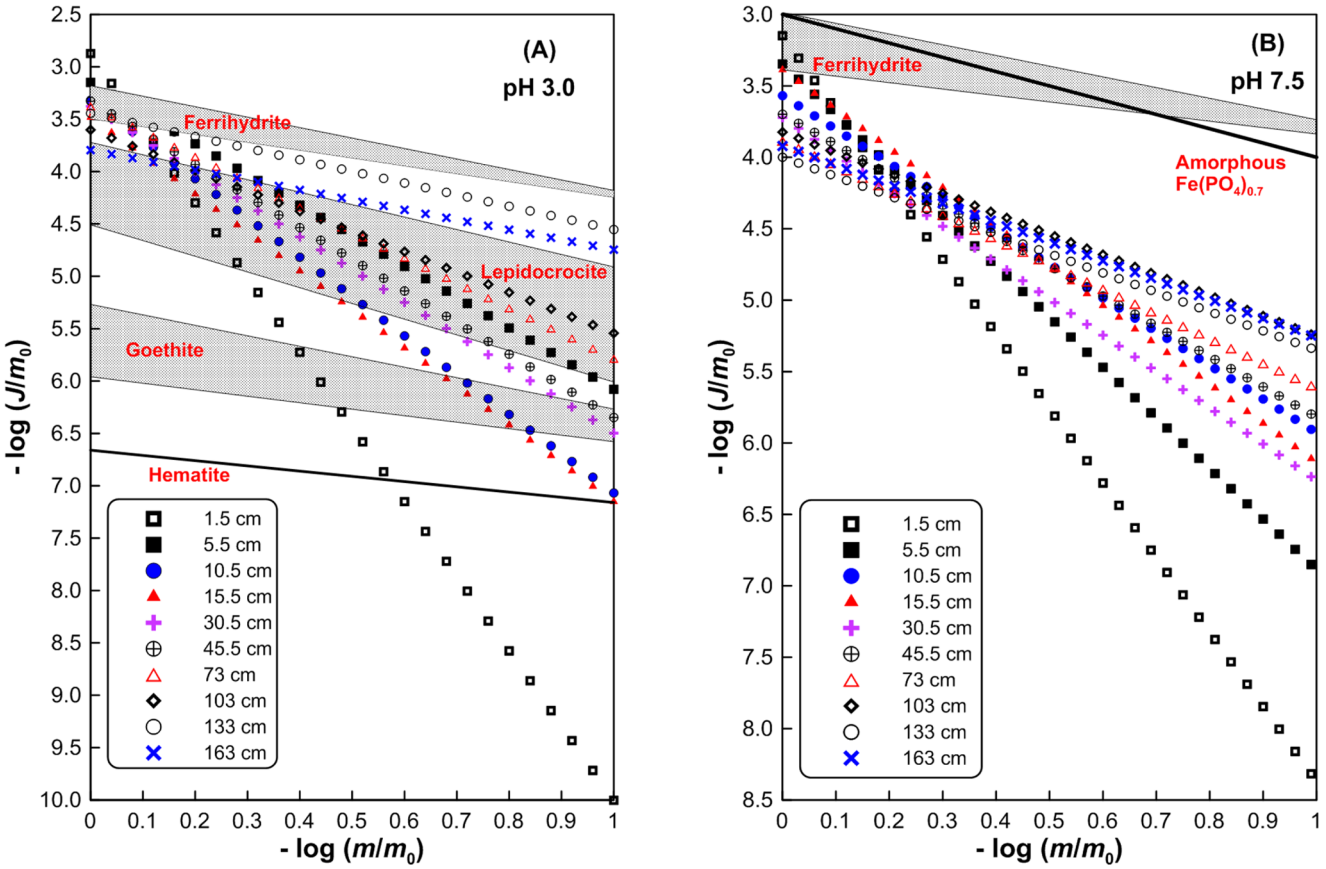

Figure 6. Reactivity of sedimentary Fe(III) oxides as compared to that of synthetic Fe(III) oxides. (A) Reduction rates at pH 3.0 normalized over initial mass (J/m_0) versus the fraction (m/m_0) remaining in the solid phase. Reactivity of ferrihydrite, lepidocrocite, goethite, and hematite at pH 3.0 is from Larsen and Postma [23] and Pedersen et al. [63,64]. (B) Reduction rates at pH 7.5 normalized over initial mass (J/m_0) versus the fraction (m/m_0) remaining in the solid phase. Reactivity of amorphous $Fe(PO_4)_{0.7}$ and ferrihydrite at pH 7.5 is from Hyacinthe and van Cappellen [28] and Raiswell et al. [29], respectively. Gray shadings in (A) and (B) delineate the ranges of Fe(III) oxide reactivity.
doi:10.1371/journal.pone.0080367.g006

moderately energetic Frisian Front and highly energetic German Bight sediments, respectively. Quick and preferential consumption of highly reactive Fe(III) oxides has left much more resistant and less heterogeneous phases (with reactivity much more resistant than or comparable to that of hematite) behind. As a result, in the deeper sediments, the decrease in dissolution rates became generally smaller relative to their initial rates. Although there is only a small variation in the initial rates (i.e., k') among the sediments at different layers, differentiating decreases in reactivity due to incongruent dissolution have resulted in a huge discrepancy (up to five and three orders of magnitude at pH 3.0 and 7.5, respectively) in dissolution rates of the residual Fe(III) oxides after dissolution of 90%. This suggests that heterogeneity has exerted a significant impact on temporal evolution of the dissolution process and dissolution rates at the later stage. This behavior may be important in controlling Fe(III) oxide dissolution in natural anoxic sediments where Fe(III) oxide reduction has proceeded to a great extent. It is worthy to point out that, the occurrence of m_0, k' and γ peaks at ~16 cm depth (with the exception of $k'(3.0)$) are probably the result of repetitive oxidation and reduction of Fe at the redox interface, which is seemingly supported by the fact that the m_0 peaks are roughly corresponding to the BCD-extractable Fe(III) peak (Fig. 2).

Selective extractions versus kinetic dissolution

Selective extractions versus $m_0(3.0)$. Both selective extraction and the reactive continuum model have been used for characterization of the reactivity of Fe(III) oxides, however, to compare the two techniques is not straightforward because the former reflects separate measurements while the kinetic parameters are derived from time-dependent experiments. Larsen et al. [21] found that $m_0(3.0)$ was only slightly higher than oxalate extractable Fe(III) but certainly lower than BCD-extractable Fe(III) in a shallow sandy aquifer (Rømø, Denmark), and thus concluded that most of the heterogeneity fell within the fraction extracted by oxalate. In the current study, the $m_0(3.0)$ is much lower than both the BCD- and oxalate-extractable Fe(III) but nearly two-fold the hydroxylamine extractable Fe(III). This suggests that the $m_0(3.0)$ cannot be quantitatively linked to any of the three selective extractions. Note that a strong linear correlation between the $m_0(3.0)$ and the BCD-extractable Fe(III) (t test, $p<0.05$) (Fig. 7A) may suggest that the $m_0(3.0)$ represents Fe(III) oxide assemblages spanning a wide spectrum of mineralogical phases from amorphous to crystalline Fe(III) oxides. This is probably the reason for the weak dependence between the $m_0(3.0)$ and the amorphous Fe(III) pool quantified by the hydroxylamine extraction (Fig. 7B). A very weak linear correlation between the $m_0(3.0)$ and the oxalate-extractable Fe(III) (t test, $p<0.05$) (Fig. 7C) is probably due to the fact that acidic oxalate can effectively

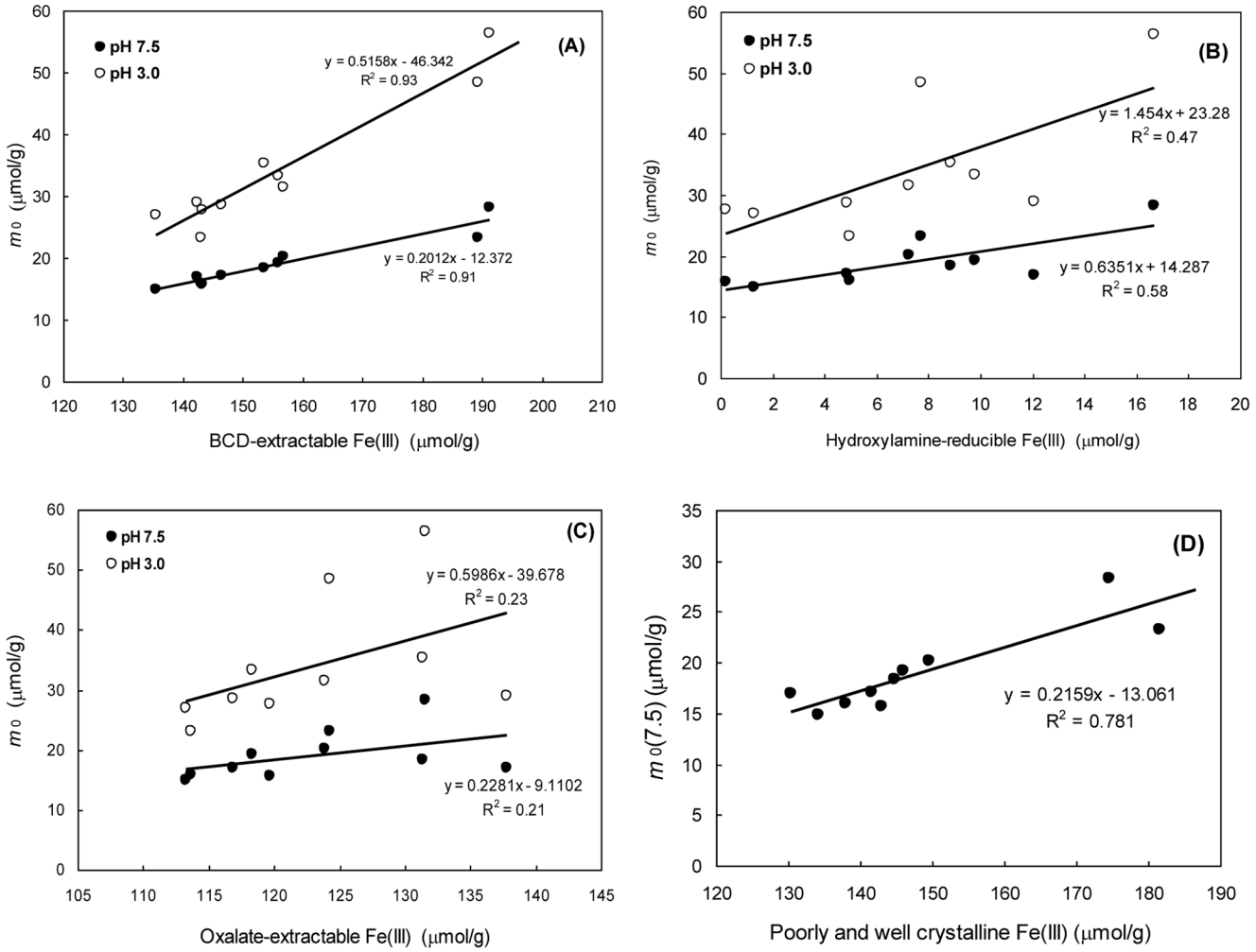

Figure 7. Correlations of extracted Fe(III) vs. three kinetic parameters. (A) BCD-extractable Fe(III) vs. m_0 at pH 3.0 and 7.5; (B) hydroxylamine-extractable Fe(III) vs. m_0 at pH 3.0 and 7.5; (C) oxalate-extractable Fe(III) vs. m_0 at pH 3.0 and 7.5; (D) poorly and well crystalline Fe(III) vs. m_0 at pH 7.5.
doi:10.1371/journal.pone.0080367.g007

dissolve magnetite but ascorbic acid at pH 3.0 cannot. In Larsen et al. [21], the rough similarity between the $m_0(3.0)$ and the oxalate-extractable Fe(III) is probably only a site-specific feature given that oxalate-extractable Fe(III) (<3 μmol/g) in the aquifer sediments was much lower than in marine sediments [43,58].

Selective extractions vs. $m_0(7.5)$. The $m_0(7.5)$ can be used as a maximum estimate of bioavailable Fe(III) present in sediments [24,28]. Hydroxylamine-extractable Fe(III) has also been used to assess the availability of Fe(III) oxides to microbial reduction, albeit being an underestimate to some extents [42]. In the present study, the hydroxylamine-extractable Fe(III) is 60−71% of the $m_0(7.5)$ in the surface/subsurface layers but decreases to 8−12% at the bottom. The larger $m_0(7.5)$ values than amorphous Fe(III) oxides quantified by the acidic hydroxylamine extraction imply that the maximum bioavailable Fe(III) (i.e., $m_0(7.5)$) should include both amorphous and other less reactive Fe(III) phases, which is seemingly supported by strong linear correlations of the $m_0(7.5)$ vs. both the BCD-extractable Fe(III) (Fig. 7A) and the amounts of poorly and well crystalline Fe(III) oxides (i.e., the difference between the BCD extraction and the hydroxylamine extraction) (*t* test, $p<0.05$) (Fig. 7D). This is in agreement with the findings that although amorphous Fe(III) oxides are always more readily susceptible to microbial reduction, iron reducers are also capable of reducing other less reactive Fe(III) oxides, even poorly reactive sheet silicate Fe(III) [59,60]. Similar to the case at pH 3.0, there is only a weak correlation between the $m_0(7.5)$ and the hydroxylamine- and oxalate-extractable Fe(III) (*t* test, $p<0.05$), respectively. Based on the analysis above, it appears that the reasons for the weak correlations between the $m_0(3.0)$ and the hydroxylamine- and oxalate-extractable Fe(III) are applicable as well to the weak correlations between the $m_0(7.5)$ and the two Fe(III) pools.

The $k'(7.5)$ can be used as a forecast proxy of maximum Fe(III) reduction rate per cell (v_{max}) based on strong linear correlation of log $k'(7.5)$ vs. logv_{max} [24]. However, the $k'(7.5)$ probably cannot directly represent the *in situ* macroscopic reactivity and initial rate of microbial Fe(III) oxide reduction in incubating and natural conditions because, by fitting available literature data of microbial Fe(III) oxide reduction to the reactive continuum model (Eq. 1), Davranche et al. [61] found that the k' was in the range of $2.2\times10^{-7}-1.85\times10^{-5}$ s^{-1}, much lower than the $k'(7.5)$ in the present study, and the γ was in the range of 5.77−44.5, higher than the present $\gamma(7.5)$. Great rate deceleration (i.e., large γ) while microbial reduction progresses in incubating and natural conditions, according to Roden [27,62], is due to adsorption of reaction products and secondary mineral formation that lead to a progressive inhibition of the reduction. In addition, microbial

reduction also exhibits very large γ in incubations which are limited by bacterial cell number [61].

It should be pointed out that only one site was used for this study, and thus spatial heterogeneity of Fe(III) oxide reactivity cannot be revealed. However, this study may have depicted a general feature of the entire inner shelf since the inner shelf (except the Yangtze Estuary) has many things in common including hydrodynamic conditions and main sediment sources. This argument is seemingly supported by generally similar diagenesis of Fe and sulfur in the northern and southern inner shelves [36,37,40,49].

Summary and Conclusion

Amorphous Fe(III) oxides were quickly consumed in the upper layer of the ECS shelf sediments but not completely depleted until at least 100-cm depth due to low availability of hydrogen sulfide towards reaction with the pool. The persistence of amorphous and poorly crystalline Fe(III) oxide pools suggests that they are readily available for quick buffering of dissolved sulfide in the sediments.

Downcore decreases in m_0, k' and γ, much quicker in the uppermost layer than at depth, indicate simultaneous decreases in content, reactivity and heterogeneity of reactive Fe(III) oxides, resulting in good linear correlations among the three kinetic parameters (except a weak correlation of $m_0(3.0)$ vs. $k'(3.0)$). Initial rates among the sediments at different depths are in a small range (within one order of magnitude), while time-dependent dissolution rate is quite different as the dissolution is in progress, which is strongly dependent on heterogeneity of Fe(III) oxides. For example, the discrepancies can reach five and three orders of magnitude at pH 3.0 and 7.5, respectively, after 90% of the Fe(III) oxides has dissolved. This behavior cannot be revealed by traditional selective extraction.

None of the three extractable Fe(III) pools is quantitatively comparable to the $m_0(3.0)$, while a strong linear correlation of the $m_0(3.0)$ vs. the BCD-extractable Fe(III) suggests that the $m_0(3.0)$ may represent Fe(III) oxide assemblages spanning amorphous and crystalline phases. Much lower amorphous Fe(III) than microbially available Fe(III) predicted by the $m_0(7.5)$ and strong linear correlations of the $m_0(7.5)$ vs. the pool of poorly and well crystalline Fe(III) oxides suggest that maximum bioavailable Fe(III) may include both amorphous and other less reactive Fe(III) phases. Although the $k'(7.5)$ can be used as a forecast proxy of maximum Fe(III) reduction rate per cell ($v_{\max}$), it cannot directly represent the *in situ* macroscopic reactivity and initial rate of microbial Fe(III) oxide reduction in natural conditions.

Acknowledgments

We thank De-Jiang Fan, Xiao-Ning Shi for their assistance of field work. Xiao-Chen Hao and Chang-Qing Fan are acknowledged for their analytical assistance. We are also grateful to three anonymous reviewers for their critical and constructive comments, which greatly helped to improve the manuscript.

Author Contributions

Conceived and designed the experiments: MXZ LJC. Performed the experiments: LJC MXZ XLH. Analyzed the data: MXZ LJC. Contributed reagents/materials/analysis tools: GPY. Wrote the paper: MXZ LJC.

References

1. Canfield DE, Thamdrup B, Hansen J (1993). The anaerobic degradation of organic matter in Danish coastal sediments: iron reduction, manganese reduction, and sulfate reduction. Geochim Cosmochim Acta 57: 3867–3883.
2. Raiswell R, Canfield DE (2012). The iron biogeochemical cycle past and present. Geochem Prospect 1: 1−220.
3. Taylor KG, Konhauser KO (2011). Iron in earth surface systems: a major player in chemical and biological processes. Elements 7: 83−88.
4. Canfield DE, Raiswell R, Bottrell S (1992). The reactivity of sedimentary iron minerals toward sulfide. Am J Sci 292: 659–683.
5. Haese RR (2006). The Biogeochemistry of Iron. In: Schulz HD, Zabel M editors. Marine Geochemistry. Berlin: Springer-Verlag. pp. 207–240.
6. Raiswell R, Canfield DE (1998). Sources of iron for pyrite formation in marine sediments. Am J Sci 298: 219−245.
7. Couture R-M, Gobeil C, Tessier A (2010). Arsenic, iron and sulfur co-diagenesis in lake sediments. Geochim Cosmochim Acta 74: 1238–1255.
8. Rozan TF, Taillefert M, Trouwborst RE, Glazer BT, Ma S, et al (2002). Iron-sulfur-phsphorus cycling in the sediments of a shallow coastal bay: implications for sediment nutrient release and benthic macroalgal blooms. Limnol Oceanogr 47: 1346–1354.
9. Gounou C, Bousserrhine N, Varrault G, Mouchel J-M (2010). Influence of the iron-reducing bacteria on the release of heavy metals in anaerobic river sediment. Water Air Soil Pollut 212: 123–139.
10. Lehtoranta J, Ekholm P, Heikki P (2009). Coastal eutrophication thresholds: a matter of sediment microbial processes. AMBIO 38: 303–308.
11. Burdige D (1993). The biogeochemistry of manganese and iron reduction in marine sediments. Earth-Sci Rev 35: 249–284.
12. Canfield DE, Kristensensen E, Thamdrup B (2005). Aquatic Geomicrobiology. Amsterdam: Elsevier. 645 p.
13. Thamdrup B (2000). Bacterial manganese and iron reduction in aquatic sediments. Adv Microbiol. Ecol 16: 41–84.
14. Aller RC, Mackin JE, Knox RT (1986). Diagenesis of Fe and S in Amazon inner shelf muds: apparent dominance of Fe reduction and implications for the genesis of ironstones. Cont Shelf Res 6: 263–289.
15. Nickel M, Vandieken V, Bruchert V, Jørgensen BB (2008). Microbial Mn(IV) and Fe(III) reduction in northern Barents Sea sediments under different conditions of ice cover and organic carbon deposition. Deep-Sea Res II 55: 2390–2398.
16. Wang Y, van Cappellen P (1996). A multicomponent reactive transport model of early diagenesis: application to redox cycling in coastal marine sediments. Geochim Cosmochim Acta 60: 2993–3014.
17. Wijsman JWM, Herman PMJ, Middelburg JJ, Soetaert K (2002). A model for early diagenetic processes in sediments of the continental shelf of the Black Sea. Estuar Coast Shelf Sci 54: 403–421.
18. Poulton SW, Krom MD, Raiswell R (2004). A revised scheme for the reactivity of iron (oxyhydr)oxide minerals towards dissolved sulfide. Geochim Cosmochim Acta 68: 3703−3715.
19. Roden EE (2003). Fe(III) oxide reactivity toward biological versus chemical reduction. Environ Sci Technol 37: 1319−1324.
20. Poulton SW, Canfield DE (2005). Development of a sequential extraction procedure for iron: implications for iron partitioning in continentally derived particulates. Chem Geol 214: 209−221.
21. Larsen O, Postma D, Jakobsen R (2006). The reactivity of iron oxides towards reductive dissolution with ascorbic acid in a shallow sandy aquifer (Romo, Denmark). Geochim Cosmochim Acta 70: 4827−2835.
22. Postma D (1993). The reactivity of iron oxides in sediments: a kinetic approach. Geochim Cosmochim Acta 57: 5027−5034.
23. Larsen O, Postma D (2001). Kinetics of reductive bulk dissolution of lepidocrocite, ferrihydrite, and goethite. Geochim Cosmochim Acta 65: 1367−1379.
24. Hyacinthe C, Bonneville S, van Cappellen P (2006). Reactive iron(III) in sediments: chemical versus microbial extractions. Geochim Cosmochim Acta 70: 4166−4180.
25. Postma D, Jessen S, Hue NTM, Duc MT, Koch CB, et al (2010). Mobilization of arsenic and iron from Red River floodplain sediments, Vietnam. Geochim Cosmochim Acta 74: 3367−3381.
26. Roden EE, Wetzel R (2002). Kinetics of microbial Fe(III) oxide reduction in freshwater wetland sediments. Limnol Oceanogr 47: 198−211.
27. Roden EE (2004). Analysis of long-term bacterial vs. chemical Fe(III) oxide reduction kinetics. Geochim Cosmochim Acta 68: 3205−3216.
28. Hyacinthe C, van Cappellen P (2004). An authigenic iron phosphate phase in estuarine sediments: composition, formation and chemical reactivity. Mar Chem 91: 227−251.
29. Raiswell R, Vu HP, Brinza L, Benning LG (2010). The determination of labile Fe in ferrihydrite by ascorbic acid extraction: methodology, dissolution kinetics and loss of solubility with age and de-watering. Chem Geol 278: 70−79.
30. Zachara JM, Kukkadapu RK, Gassman PL, Dohnalkova A, Fredrickson JK, et al (2004). Biogeochemical transformation of Fe minerals in a petroleum-contaminated aquifer. Geochim Cosmochim Acta 68: 1691−1700.
31. Liu JP, Xu KH, Li AC, Milliman JD, Velozzi DM, et al. (2007). Flux and fate of Yangtze River sediment delivered to the East China Sea. Geomorphology 85: 208–224.

32. Wang X-C, Sun M-Y, Li A-C (2008). Contrasting chemical and isotopic compositions of organic matter in Changjiang (Yangtze River) esturine and East China Sea shelf sediments. J Oceanogr 64: 311–321.
33. Xu K, Milliman JD, Li A, Liu JP, Kao S-J, et al (2009). Yangtze- and Taiwan-derived sediments on the inner shelf of East China Sea. Cont Shelf Res 29: 2240−2256.
34. Zhao Y-Y, Yan M-C, Jiang R-H (1995). Abundance of chemical elements in continental shelf sediment of China. Geo-Mar Lett 15: 71−76.
35. Zhu M-X, Hao X-C, Shi X-N, Yang G-P, Li T (2012). Speciation and spatial distribution of solid-phase iron in surface sediments of the East China Sea continental shelf. Appl Geochem 27: 892−905.
36. Huang K-M, Lin S (1995). The carbon-sulfur-iron relationship and sulfate reduction rate in the East China Sea continental shelf sediments. Geochem J 29: 301–315.
37. Lin S, Huang K-M, Chen S-K (2000). Organic carbon deposition and its control on iron sulfide formation of the southern East China Sea continental shelf sediments. Cont Shelf Res 20: 619–635.
38. Lin S, Huang K-M, Chen S-K (2002). Sulfate reduction and iron sulfide mineral formation in the southern East China Sea continental slope sediment. Deep-Sea Res I 49: 1837–1852.
39. Bao G-D (1989). Separation of iron and manganese in the early diagenetic processes and its mechanism of biogeochemistry. Sci. China (Ser. B) 19: 93–102 (in Chinese).
40. Liu J, Zhu M-X, Yang G-P, Shi X-N (2013). Quick sulfide buffering in inner shelf sediments of the East China Sea impacted by eutrophication. Environ. Earth Sci DOI: 10.1007/s12665-013-2454-4.
41. Lü R-Y, Zhu M-X, Li T, Yang G-P, Deng F-F (2011). Speciation of solid-phase iron in mud sediments collected from the shelf of the East China Sea: Constraints on diagenetic pathways of organic matter, iron, and sulfur. Geochimica. 40: 363–371 (in Chinese with English abstract).
42. Lovley DR, Phillips EJP (1987). Rapid assay for microbially reducible ferric iron in aquatic sediments. Appl Environ Microbiol 53: 1536–1540.
43. Kostka J, Luther GW (1994). Partitioning and speciation of solid phase iron in saltmarsh sediments. Geochim Cosmochim Acta 58: 1701–1710.
44. de Koff JP, Anderson MA, Amrhein C (2008). Geochemistry of iron in the Salton Sea, California. Hydrobiologia 604: 111−121.
45. Mehra OP, Jackson ML (1960). Iron oxide removal from soils and clays by a dithionite–citrate system buffered with sodium bicarbonate. Clays Clay Miner 7: 317–327.
46. Lord CJ (1982). A selective and precise method for pyrite determination in sedimentary materials. J Sediment Petrol 52: 664–666.
47. Raiswell R, Canfield DE, Berner RA (1994). A comparison of iron extraction methods for the determination of degree of pyritisation and the recognition of iron-limited pyrite formation. Chem Geol 111: 101−110.
48. Stookey LL (1970). Ferrozine—a new spectrophotometric reagent for iron. Anal Chem 42: 779−781.
49. Aller RC, Mackin JE, Ullman WJ, Wang C-H, Tsai S-M, et al. (1985). Early chemical diagenesis, sediment-water solute exchange, and storage of reactive organic matter near the mouth of the Changjiang, East China Sea. Cont Shelf Res 4: 227–251.
50. Zhu M-X, Shi X-N, Yang G-P, Hao X-C (2013). Formation and burial of pyrite and organic sulfur in mud sediments of the East China Sea inner shelf: constraints from solid-phase sulfur speciation and stable sulfur isotope. Cont Shelf Res 54: 24−36.
51. Canfield DE, Berner RA (1987). Dissolution and pyritization of magnetite in anoxic marine sediments. Geochim Cosmochim Acta 51: 645–659.
52. Leslie BW, Hammond DE, Berelson WM Lund SP (1990). Diagenesis in anoxic sediments from the California continental borderland and its influence on iron, sulfur, and magnetite behavior. J Geophys Res 95: 4453–4470.
53. Giordani G, Azzoni R, Viaroli P (2008). A rapid assessment of the sedimentary buffering capacity towards free sulphides. Hydrobiologia 611: 55–66.
54. Zhu M-X, Liu J, Yang G-P, Li T, Yang R-J (2012). Reactive iron and its buffering capacity towards dissolved sulfide in sediments of Jiaozhou Bay, China. Mar Environ Res 80: 46−55.
55. van der Zee C, van Raaphorst W (2004). Manganese oxide reactivity in North Sea sediments. J Sea Res 52: 73−85.
56. DeMaster DJ, McKee BA, Nittrouer CA, Jiangchu Q, Guodon C (1985). Rates of sediment accumulation and particle reworking based on radiochemical measurements from continental shelf deposits in the East China Sea. Cont Shelf Res 4: 143–158.
57. Weiss JV, Emerson D, Megonigal JP (2004). Geochemical control of microbial Fe(III) reduction potential in wetlands: comparison of the rhizosphere to non-rhizosphere soil. FEMS Microbiol Ecol 48: 89–100.
58. Canfield DE (1989). Reactive iron in marine sediments. Geochim Cosmochim Acta 53: 619–632.
59. Dong H, Jaisi DP, Kim J, Zhang G (2009). Microbe-clay mineral interactions. Am Mineral 94: 1505–1519.
60. Roden EE, Zachara JM (1996). Microbial reduction of crystalline iron(III) oxides: influence of oxide surface area and potential for cell growth. Environ Sci Technol 30: 1618–1628.
61. Davranche M, Dia A, Fakih M, Nowack B, Gruau G, et al. (2013). Organic matter control on the reactivity of Fe(III)-oxyhydroxides and associated As in wetland soils: a kinetic modeling study. Chem Geol 335: 24−35.
62. Roden EE (2006). Geochemical and microbiological controls on dissimilatory iron reduction. C R Geosci 338: 456−467.
63. Pedersen HD, Postma D, Jakobsen R, Larsen O (2005). Fast transformation of iron oxyhydroxides by the catalytic action of aqueous Fe(II). Geochim Cosmochim Acta 69: 3967−3977.
64. Pedersen HD, Postma D, Jakobsen R (2006). Release of arsenic associated with the reduction and transformation of iron oxides. Geochim Cosmochim Acta 70: 4116−4129.